



THE UNIVERSITY *of* EDINBURGH

## Edinburgh Research Explorer

### Do blue-ice moraines in the Heritage Range show the West Antarctic ice sheet survived the last interglacial?

**Citation for published version:**

Fogwill, CJ, Hein, AS, Sugden, DE & Bentley, MJ 2012, 'Do blue-ice moraines in the Heritage Range show the West Antarctic ice sheet survived the last interglacial?', *Palaeogeography, Palaeoclimatology, Palaeoecology*, vol. 335-336, pp. 61-70. <https://doi.org/10.1016/j.palaeo.2011.01.027>

**Digital Object Identifier (DOI):**

[10.1016/j.palaeo.2011.01.027](https://doi.org/10.1016/j.palaeo.2011.01.027)

**Link:**

[Link to publication record in Edinburgh Research Explorer](#)

**Document Version:**

Peer reviewed version

**Published In:**

Palaeogeography, Palaeoclimatology, Palaeoecology

**Publisher Rights Statement:**

This is the author's version of a work that was accepted for publication. Changes resulting from the publishing process, such as peer review, editing, corrections, structural formatting, and other quality control mechanisms may not be reflected in this document. Changes may have been made to this work since it was submitted for publication. A definitive version was subsequently published in Palaeogeography, Palaeoclimatology, Palaeoecology (2012)

**General rights**

Copyright for the publications made accessible via the Edinburgh Research Explorer is retained by the author(s) and / or other copyright owners and it is a condition of accessing these publications that users recognise and abide by the legal requirements associated with these rights.

**Take down policy**

The University of Edinburgh has made every reasonable effort to ensure that Edinburgh Research Explorer content complies with UK legislation. If you believe that the public display of this file breaches copyright please contact [openaccess@ed.ac.uk](mailto:openaccess@ed.ac.uk) providing details, and we will remove access to the work immediately and investigate your claim.



# Do blue-ice moraines in the Heritage Range show the West Antarctic Ice Sheet survived the last interglacial?

Christopher J. Fogwill\*, Andrew S. Hein, Michael J. Bentley and David E. Sugden

\*Corresponding Author

This is the author's final draft as submitted for publication. The final version was published in *Palaeogeography, Palaeoclimatology, Palaeoecology* by Elsevier (2012)

Cite As: Fogwill, CJ, Hein, AS, Sugden, DE & Bentley, MJ 2012, 'Do blue-ice moraines in the Heritage Range show the West Antarctic ice sheet survived the last interglacial?' *Palaeogeography, Palaeoclimatology, Palaeoecology*, vol 335-336, pp. 61-70.

DOI: 10.1016/j.palaeo.2011.01.027

Made available online through Edinburgh Research Explorer

# **Do blue-ice moraines in the Heritage Range show the West Antarctic Ice Sheet survived the last interglacial?**

Christopher J. Fogwill<sup>1</sup>, Andrew S. Hein<sup>2</sup>, Michael J. Bentley<sup>3</sup>, David E. Sugden<sup>2</sup>

<sup>1</sup>School of Geography, University of Exeter, Streatham Campus, Northcote House, Exeter, EX4 4QJ, UK. Email: C.J.Fogwill@exeter.ac.uk

<sup>2</sup>School of GeoSciences, University of Edinburgh, Edinburgh, EH8 9XP, UK.

<sup>3</sup>Department of Geography, University of Durham, Durham, DH1 3LE, UK.

## **Abstract**

We present a hypothesis that best explains cosmogenic isotope data on blue-ice moraines in the Heritage Range, West Antarctica. The age of the moraines implies that they, and the related ice-sheet surface with which they are associated, have persisted on the flanks of nunataks throughout at least the last interglacial/glacial cycle. The implication is that although the West Antarctic Ice Sheet (WAIS) may have fluctuated in thickness during glacial cycles, the central dome has remained intact for at least 200 kyr and possibly even for 400 kyr. Such a finding, if substantiated, would contribute to our understanding of the sensitivity of the West Antarctic Ice Sheet to climate change. Further it would be a powerful geomorphic constraint on models of the past behaviour of the ice sheet during glacial cycles and thus those predicting the future of the ice sheet in a warming world.

## Keywords

Blue-ice moraine West Antarctic Ice Sheet Geomorphology Last Glacial cycle

## 1. Introduction

This purpose of this paper is to develop a hypothesis that best explains geomorphological observations and cosmogenic nuclide data on moraines in the Patriot Hills, southern Heritage Range, West Antarctica (Fig. 1). The data was collected as part of a project seeking to establish the magnitude of ice-sheet thinning since the Last Glacial Maximum (LGM). Using morphology and the highest post-LGM dates as a guide, the project established post LGM thinning of 230-480m in the Patriot Hills (Bentley *et al.*, 2010). The project also encountered a puzzle that has faced the field of exposure-age dating more widely in Antarctica. The exposure-age dating revealed an upper limit of unweathered deglacial boulders exposed ~ 15 ka years ago, reflecting the thickness of the ice during the LGM. But, in common with several other studies of the former thickness of the ice sheet during the LGM, the samples were mixed with much older samples which have been exposed for up to several hundred thousand years (Ackert *et al.*, 1999; Sugden *et al.*, 2005; Fink *et al.*, 2006; Mackintosh *et al.*, 2007). It has been common to assume, and sometimes can be demonstrated, that the latter have a complex burial history and have been reworked by the glacier. However, the co-isotopic data in the Patriot Hills are consistent with an alternative hypothesis, namely that the spread of ages on blue ice moraines and nunatak slopes reflects the length of time that the moraine and the adjacent ice margin has been continuously present. In such a case, new clasts constantly accumulate on the glacier surface and are added to the moraine to build a deposit with a range of exposure ages. As the ice thickness fluctuates during glacial cycles part of this deposit with mixed ages is deposited on the mountain fronts. Clearly, if substantiated, such a hypothesis offers a new way of studying West Antarctic ice-sheet stability over glacial cycles.

The hypothesis must be viewed as unsubstantiated in that the moraines were sampled with a different aim in mind and the supportive data is no more than indicative. A rigorous examination of the process and a detailed programme of dating are required to test the hypothesis. At this stage the potential importance of the hypothesis and the approach it opens up is the justification for this paper.

## **2. Background**

Understanding the behaviour of the West Antarctic Ice Sheet is important. It is a marine-based ice sheet with its centre situated on bedrock which is below sea level. As glaciological theory and study of northern hemisphere deglaciation showed in the 1970s, this introduces a potential instability that can lead to rapid collapse (Weertman, 1974, Mercer, 1978). The crucial unknown is how floating ice shelves, which have a buttressing effect on ice streams, respond to sea-level change and ocean melting. The risk is that the volume of ice, if lost, would be sufficient to raise eustatic sea level by 5 m if all the ice disappeared or by 3.3 m if icecaps remained on the main mountain blocks (Bamber *et al.*, 2009).

Several attempts to model the effects of such changes have reinforced the view that the ice sheet is sensitive to ocean change. Warner and Budd (1998) showed that basal melting was the dominant factor for the future health of the ice sheet and that a rise in water temperature of only 3° C could set in chain a process that could remove the ice sheet within 2,000 years. Ritz *et al.* (2001) and Huybrechts (2002), parameterising the grounding line and ice shelves in different ways, ran ice-sheet models over the last 400,000 years and suggested that during the last interglacial at ~125 kyr the WAIS was either much smaller than present or had collapsed. Pollard and DeConto (2009) introduced a new approach to grounding-line dynamics and ice-shelf buttressing (Schoof, 2007) and ran an ice sheet model for 5 million years, forced mainly by ocean warming linked to a stacked deep-sea-core benthic  $\delta^{18}\text{O}$  record. The WAIS disappeared at MIS 31 (1.07 Myr) and in a Pleistocene interval at ~200 kyr.

The sensitivity of the WAIS to warming has been bolstered by far-field evidence in the form of high eustatic sea levels, especially during the last interglacial (MIS 5e, (120 kyr)). Since Hollin (1965) suggested that high interglacial sea levels may partly reflect the collapse of the WAIS, there has been support for such an idea from the dating of fossil corals (McCulloch and Esat, 2006) and from high-resolution  $\delta^{18}\text{O}$  records from marine sedimentary cores (Siddall *et al.*, 2003). High sea levels are known from both the last interglacial (Hearty, *et al.*, 2007, Rohling *et al.*, 2008) and earlier interglacials such as MIS 9 (330 kyr) (Hearty, 1998) and MIS 11 (400 kyr) (Raynaud, 2003). In such cases there is often evidence of global temperatures warmer than present and the loss of the WAIS, along with Greenland, is seen as a possible source of the additional water required (Kopp *et al.*, 2009).

Evidence within Antarctica has also been interpreted in terms of a sensitive WAIS that can disappear in interglacials. Such a case has been made on the basis of Quaternary and Tertiary microfossils found beneath ice streams flowing into the Ross Ice Shelf (Scherer, 1991), and more recently on the basis of diatom oozes of Pliocene age discovered beneath the Ross Ice Shelf by the ANDRILL coring programme (Naish *et al.*, 2009). The oozes demonstrate open water and warmer conditions in the western Ross Sea when planetary temperatures were up to 3°C warmer than today. The interpretation is that at such times the WAIS, the main source of ice into the Ross Ice Shelf, had largely disappeared.

There is empirical evidence of WAIS sensitivity during the last glacial cycle from the peripheries of the ice sheet. The ice sheet has diminished in size from the Last Glacial Maximum (LGM) in all sectors. The biggest changes occur in the Pacific sector of the Ross and Amundsen Seas. The grounding line of the Ross Ice Shelf has retreated by ~800 km since the LGM (Conway *et al.*, 1999). Holocene thinning of 800 m linked to grounding-line retreat has been established by exposure-age dating in Marie Byrd Land (Stone *et al.*, 2003). A submarine landform record of a 130-km retreat of a grounded ice sheet has been identified in the Amundsen Sea embayment (Anderson *et al.*, 2002; Graham *et al.*, 2009) and retreat of the grounding line and rapid thinning of outlets, such as Pine Island Glacier, continues to this day, extending some 150 km inland (Shepherd *et al.*, 2001; Pritchard *et al.*,

2009). In the Weddell Sea sector, there is surface exposure-age evidence for thinning of 230-480 m (Bentley *et al.*, 2010), a modest figure that agrees with the conclusion that the low-lying Berkner Island at the ice front of the Filchner-Ronne Ice Shelf was not overridden by the ice sheet at the Last Glacial Maximum (Mulvaney *et al.*, 2007). Overall the evidence from the WAIS peripheries is consistent with the view that the ice sheet is changing from glacial to an interglacial state and that the response is not yet complete.

### **3. Blue ice moraines**

Bearing in mind the importance of assessing the sensitivity of the WAIS and its role in sea-level change, and the uncertainty associated with different approaches, it seems worthwhile exploring alternative lines of attack. The identification of the long-lived nature of blue-ice moraines opens up just such a new possibility.

Blue-ice areas cover ~120,000 km<sup>2</sup> of Antarctica where they indicate zones of ablation by wind and sublimation (Bintanja, 1999; Winther *et al.*, 2001; Sinisalo and Moore, 2010). Blue ice is found in areas where winds are focussed by steeper surface slopes or where topography concentrates air flow in depressions or in the vicinity of nunataks. Since ice flow compensates for the surface ablation, deeper, older ice rises to the surface where it is exposed in the typically rippled blue ice surface. Some of the exposed ice may range from zero to hundreds of thousands of years old. These latter characteristics help explain why blue ice areas are such suitable locations for collecting meteorites that fall on upstream zones of the ice sheet, at least in East Antarctica (Whillans and Cassidy, 1983; Yoshida *et al.*, 1971). In certain nunatak areas moraines are associated with blue ice at or near the glacier margin, as for example, in the Ellsworth massif, Lambert basin, Dronning Maud Land and the Transantarctic Mountains. If such moraines are found to be long lived and can be dated, then they and relict deposits on nunatak slopes hold the potential to track changes in the former thickness of the ice sheet over time at many different inland locations. Such information, distributed around Antarctica, would be of great value to modellers seeking to refine and constrain ice-sheet models.

### 3.1 Blue-ice moraines in the Heritage Range

The Heritage Range is in a key location to record the behaviour of the central dome of the West Antarctic Ice Sheet. Outlet glaciers flowing around the nunataks drain the central dome of the WAIS, and yet the innermost grounding line of the Filchner-Ronne Ice Shelf is only 50 km distant. The mountains lie across the main flow of the ice sheet and as a result altitudes are higher on the inland flank (~1200 m) than on the coastal side (~800 m). In this paper we record blue-ice moraines on Soholt Peaks and the Liberty Hills but focus our field observations on the Independence, Marble and Patriot Hills. In the latter three locations ice spills over the escarpments from the interior into Horseshoe Valley, a trough with a glacier 1500 m deep and flowing in a trough 700 m below sea level (Casassa *et al.*, 2004).

The Ellsworth Mountains constitute an isolated mountain block that is composed of some 13,000 m of sedimentary rocks that form an almost complete succession from the Late Cambrian to The Permian (Webers *et al.* 1992). The succession includes numerous lithological boundaries and this variety through the sequence allows us to identify local or far-travelled glacial erratics and to infer regional ice dynamics. In the Heritage Range the bedrock is primarily composed of marble and limestone conglomerates of the Union Glacier Formation, which are overlain by greywackes and conglomerates, shales and argillites of the Hyde Glacier and Drake Icefall Formations. This succession is overlain by quartzites of the Minaret Formation in the Heritage Range and the Crashite Group which outcrop in the Sentinel Range to the north.

The mean annual temperature is estimated to be  $-28^{\circ}\text{C}$  on the basis of a 10 m borehole at Patriot Hills (Dahe *et al.*, 1994). The accumulation rate has been estimated to be 0.2-0.3 m a<sup>-1</sup> of water equivalent (Genthon and Braun, 1995). Katabatic winds from the ice-sheet interior cross the axis of the escarpment and ablate ice from the ice margin at the foot of the escarpment. Ablation is concentrated at the ice margin which is lower than the axis of the trunk glacier. On the basis of local measurements



in 1996-1997 (Casassa *et al.* 2004) and altitudinal relationships elsewhere in Antarctica (Bintanja, 1999; Näslund, 1992), the rate of ice ablation is likely to be 15-20 cm water equivalent per year

Blue-ice moraines occur at the foot of several mountain escarpments. At the foot of Soholt Peaks are two prominent moraines up to 20 m high and 150-200 m broad. There is also a narrower blue-ice moraine extending 3 km downstream of the confluence of Schanz Glacier and ice from Drake Icefall (Fig. 2). Blue-ice moraines extend relatively continuously along the foot of the escarpment of the Liberty Hills for several km, often cutting across local glaciers situated on the slope. At Independence Hills there is a sequence of over 10 closely spaced parallel moraines at the foot of a 500 m escarpment. The moraines are up to 10 m high, each a few tens of m across, and extend for some 4 km (Fig. 3). The moraines are hooked in planform and each has an onset immediately downstream of spurs in the escarpment. Several of the moraines are virtually monolithologic with most clasts similar to that of the spur at their onset. Because of the along-strike variation in the geology of the hills, there are marked differences in lithologic composition of adjacent moraines. At the foot of the Patriot Hills is a blue ice moraine up to 20 m high, 220 m across extending over 4 km along the escarpment front before swinging northwards to the coast. The moraine contains lithologies that are exotic to the massif. Relict moraines occur on the escarpment front up to 250 m above the glacier. It is in this latter area that we focussed our cosmogenic nuclide study.

### **3.2 The Patriot Hills blue-ice moraines**

#### *3.2.1. Morphology and sediments*

The Patriot Hills escarpment, formed by shale, marl limestone and argillites, has summits of around 1200 m with slopes of ~28° overlooking Horseshoe Glacier at its foot at 770 m. The front is scalloped with embayments, some holding local glaciers that extend down to the main glacier. The blue-ice moraine is continuous for over 4 km and is widest in embayments where there are no local glaciers (Fig. 4). Figure 5 shows a transect (surveyed with a handheld level) through the largest expanse. The main deposit consists of a ridge of sub-parallel ridges of boulders and gravel, often one clast thick,

overlying ice. Approximately 80% of the material consists of local lithologies but 20% consists of varied lithologies exotic to the massif, mainly sandstone and quartzite. The moraine stands 20 m above the adjacent exposed glacier surface but is at a similar altitude to the trunk glacier surface 1 km distant. The glacier surface slopes towards the margin at the escarpment foot at  $\sim 6^\circ$ . At the edge of the exposed glacier surface are debris bands, typically 0.3-1.5m wide dipping towards the trunk glacier at angles of  $70-80^\circ$ . Some contain clasts aligned parallel to the band and protruding above the surface (Fig. 6). In plan view the debris bands are parallel to the ice edge but in detail they are discontinuous and frequently zigzag with sharp reversals of orientation. Figure 5 also shows a transect across the blue-ice moraine and onto a local debris-covered glacier. Here is the same pattern of debris bands dipping towards the main trunk glacier and exotic boulders, some of which are clearly striated, at the edge of the blue ice zone. This contrasts with the local glacier which has white bubbly ice with foliations dipping in the opposite direction towards the escarpment and the whole covered in local angular marl clasts.

There are relict moraines with distinct ridge morphology distributed across the slopes of the escarpment up to 230-250 m above the present glacier. They are parallel to the ice edge and often part of a more continuous till cover with a light brown gravel matrix. The uppermost tills contain a mix of a few weathered and abundant unweathered clasts of sandstone, quartzite, volcanics and limestone, up to  $\sim 20\%$  of which are exotic. The variety of lithologies increases at lower altitudes and some clasts at all levels are striated. Limestone boulders mostly  $< 0.5$  m, but up to 4 m in diameter, can be traced to local rock outcrops to the immediate southwest. At its upper limit the zone of morphologically distinct moraines onlaps onto a 30 m altitudinal zone (240-280 m above the glacier) of weathered till patches with deeply weathered, iron-stained sandstone, quartzite, limestone and volcanics. Former basalt boulders are shattered and some volcanic clasts 30 cm in diameter have been weathered to the soil surface level. There are no unweathered clasts. Above this and at more than 280 m above the glacier are exposed bedrock surfaces with only occasional isolated erratics of weathered and iron-stained sandstones, limestone and volcanics.

### 3.2.2. Cosmogenic isotope analysis

Initial cosmogenic  $^{10}\text{Be}$  and  $^{26}\text{Al}$  analyses of 28 samples provides quantitative constraints on the age of both the current and past moraines in front of the Patriot Hills (Fig. 7 and Table 1). In addition, we took four samples from blue-ice moraines in the Independence Hills and further samples from till deposits in the neighbouring Marble Hills. We preferentially sampled quartz-rich erratics, including quartzites, sandstones, granitic lithologies and some metasediments from ice-free bedrock and till-covered surfaces. Samples varied from small cobbles (~15 cm long axis) through to large boulders (~1m<sup>2</sup>). For larger erratics, we sampled the upper surface to ensure maximum possible cosmogenic isotope production and minimal snow cover throughout the exposure period.  $^{10}\text{Be}$  was selectively extracted from the quartz component of the whole rock sample, following Ivy-Ochs (1996), and using the standard procedures at the University of Edinburgh Cosmogenic Isotope Laboratory. Apparent exposure ages (Table 1) were generated using a  $^{10}\text{Be}$  production rate scaled to sea level high latitude (SLHL) in Antarctica using the CRONUS-Earth Online calculator of Balco *et al.* (2008).

The  $^{10}\text{Be}$  results show that two clasts emerging from and on the glacier surface in the Patriot Hills have experienced virtually no exposure to the atmosphere. Three clasts on the current ice-cored moraine have exposure ages of 31-44 kyr. On a current blue-ice moraine in the nearby Independence Hills the three sample ages range from 1-28 kyr. In the Patriot Hills four weathered and iron-stained clasts from the uppermost weathered moraine deposits at ~ 230-250 m yield a cluster of exposure ages around 400 kyr (400-445 kyr). The deposits containing freshly weathered clasts yield 13 ages of 3.0-77.0 kyr. In the neighbouring Marble Hills the equivalent upper limit of freshly weathered clasts yields two youngest ages of 15 kyr along with older, reworked clasts (Bentley *et al.*, 2010).

The results of subsequent analysis of  $^{26}\text{Al}$  from the elevated blue-ice deposits on the escarpment front are also shown for the Patriots in Fig. 7. In 7 out of 8 cases, and ranging from 14-50 kyr, the aluminium results are the same (within error) as the beryllium ages. In the one remaining co-isotopic case (CF-13-08) the difference is marginal. We also carried out  $^{26}\text{Al}$  analysis on a high-level clast in

the Marble Hills with a  $^{10}\text{Be}$  age of  $205.6 \pm 19.6$  kyr and it yielded a similar  $^{26}\text{Al}$  age within error, namely  $197.9 \pm 19.4$  kyr.

#### 4. Discussion

The geomorphological observations in the Patriot Hills give some clues as to the processes involved in blue-ice moraine formation, while the cosmogenic results provide perspective on their long-term evolution. In a nutshell, the hypothesis is that these blue-ice moraines are equilibrium forms caused by localised ablation bringing local and far-field basal material to the surface. Moreover, they can persist for hundreds of thousands of years, migrating up and down the escarpment front in response to thickness changes during glacial cycles.

##### 4.1 Process

A key requirement is a process whereby material from the base of the glacier can accumulate on the glacier surface and not be removed by lateral flow. At first sight of blue-ice moraines, especially from the air, the impression is of lateral and medial moraines deriving rock material from rocky outcrops and flowing downglacier. With such a viewpoint it would be unlikely that any moraine could persist for long before being evacuated from the continent. The crucial requirement for equilibrium is for compressive ice flow towards the margin of the glacier capable of bringing basal material to the surface and retaining it there. The field evidence supports just such a scenario. The ice surface gradient slopes towards the ice margin with a slope of around  $6^\circ$  and an amplitude of some 30 m in the kilometre closest to the margin. This is sufficient to provide compressive flow at right angles to the glacier margin. The dip and zigzag pattern of the debris bands is typical of ice deformation and folding known to characterize the compressive marginal zone. The striations, the varied size of debris, varying from dust to boulders, and especially the orientation of the latter parallel to the dirt band are typical of basally derived debris bands (Sugden *et al.* 1987). Finally, the  $^{10}\text{Be}$  analyses on two clasts picked randomly from the ice surface show no exposure to cosmic rays, something that would be expected had the clasts only recently arrived at the surface having been eroded at the glacier base.

A second process is necessary to concentrate the debris into moraines. This will result from katabatic winds sweeping down the escarpment and causing ablation. Ablation removes ice at the expense of rock debris, while ice flow compensates for ablation and concentrates the clasts towards the ice margin. When the debris cover is sufficiently thick, it cuts off ablation, and hence the creation of a protected moraine-covered ice ridge standing above the bare glacier surface. Such a process of concentration of rock debris by ablation, preserving the underlying ice for millions of years, has been described in Beacon Valley in the Transantarctic Mountains of southern Victoria Land (Kowalewski *et al.*, 2006). In the case of the Patriot Hills the moraine crest is no higher than the elevation of the main trunk glacier. It is difficult to judge the relative importance of ice flow at right angles to the margin or lateral to it. The link of some rock types to particular outcrops argues for some lateral movement or a source of local ice joining the main glacier as in the Independence Hills. However, the high volumes of material in embayments argues for debris retention and ice flow towards the margin with little or no lateral component. Here is a clear need for detailed field measurements of ice flow in the vicinity of the blue-ice moraines.

Little can be said about the rate of blue-ice moraine formation. Nonetheless even crude comparisons of the sparse amount of debris arriving at the ice surface and the large volumes that have accumulated in the large embayment (Figs 4 & 5), suggests that the process of concentration has been continuing for many tens of thousands of years. Such a conclusion is backed up by the exposure age of three boulders on the ice-cored moraine in the Patriots of 31-44 kyr and a further age from the ice-cored moraines in the Independence Hills of 28 kyr.

#### *4.2. Long term evolution*

On the basis of the above and the wider pattern of surface exposure ages, Bentley *et al* (2010) have interpreted the upper limit of freshly weathered clasts as the elevation of the ice sheet surface during the LGM. They assumed that the older ages below the limit represented complex exposure histories and that old clasts had been reworked.

But the co-isotopic work using  $^{26}\text{Al}$  on some of the samples, suggests something more interesting. In many cases the similarity of the beryllium and aluminium ages suggests a simple exposure history. In other words some clasts have been exposed to cosmic rays for tens or even hundreds of thousands of years and have not been buried or reworked by the ice. The agreement is particularly marked below the presumed LGM limit in the Patriot Hills containing unweathered clasts. Intriguingly it also includes a high-level clast in the Marble Hills with beryllium and aluminium ages of 205 kyr and 198 kyr respectively. This latter clast has been exposed continuously to cosmic rays since the penultimate glaciation. At present there are insufficient co-isotopic data from the uppermost clasts with exposure ages of 400-kyr to make meaningful interpretations. Experience in the Shackleton Range shows that, when the effects of erosion are borne in mind, such beryllium and aluminium ages may in reality be much older (Fogwill *et al.*, 2004).

A notable feature of the moraine deposits is their continuity, not only in their ridge morphology but also in the similarity of the sediments and the lithological mix of the quartzite, sandstone and limestone exotic erratics. The main differences are in terms of weathering and the apparent loss by weathering of less resistant rock types in the uppermost weathered zone. The varying proportions of weathered clasts in the upper moraines, and the mix and span of ages suggests that the ice reached similar altitudes on several occasions.

#### *4.3. Refining the hypothesis*

The simplest hypothesis to explain the continuity and exposure-age results is that the blue-ice moraines migrate up and down the escarpment front during glacial cycles (Fig. 8). During glacial cycles when global sea level falls, the grounding line migrates seawards and the ice thickens by 230-280 m. During interglacials, sea level rises, the grounding line retreats landwards, and the ice thins in response. As the ice margin migrates up and down the escarpment the glacier deposits clasts with a span of ages. Many will have been exposed to cosmic rays continuously, while some disturbed during the process may have more complex histories. In the case of the Patriot and Marble Hills, the

evidence within the zone of mixed young and old clasts points to stability for at least 200 kyr.

However, the exposure ages of 400 kyr in the Patriot Hills could imply an even longer history of stability.

It has been suggested that we cannot rule out the possibility that individual clasts remained exposed on nunataks continuously through a period of ice sheet collapse during an interglacial and that such clasts were picked-up during ice-sheet re-growth and redeposited with an undetectably short period of re-burial. We agree that such a possibility cannot be ruled out at this stage. However, the lithological and morphological continuity of the deposits and the number of clasts that we have detected with continuous exposure histories argues against such a collapse-regrowth scenario. This problem of ice-sheet stability requires further work and the use of different isotopes to reach a firmer conclusion.

Our hypothesis helps explain several puzzles. First, it explains the sheer size of the moraines which simple calculations suggest must represent many thousands of years of accumulation of the sparse density of clasts arriving at the ice surface. Second, it explains the spread of exposure ages with simple exposure histories. It could also help explain some of the older exposure ages so frequently obtained below the LGM limit elsewhere in Antarctica. Indeed, one can speculate that moraines often represent former blue-ice ablation areas and these sites open up windows into the deeper history of the Antarctic ice sheet. Perhaps too the converse is true; the most recent history may be best retrieved from erratics sparsely distributed on bedrock surfaces distant from moraine accumulations.

Finally, the hypothesis has a wider significance. Bearing in mind the location of the southern Heritage Range on the border of the central dome of the WAIS, these conclusions about blue-ice moraine stability may carry the important implication that the central ice-sheet dome did not disappear during the last interglacial. It remains to reconcile this conclusion with other lines of evidence outlined earlier in the paper pointing to the disappearance of the WAIS during the last interglacial. Perhaps it is the underlying topography that helps make the central core of the WAIS and the Weddell Sea sector sufficiently stable to have survived the last interglacial.

## **5. Conclusion**

These initial results suggest that blue-ice moraines in the Heritage Range have the potential to provide direct evidence of whether or not the WAIS survived the last interglacial. Furthermore, analysis of the upper weathered deposits could open up an even deeper terrestrial window of at least 400 kyr into the history of the WAIS, perhaps indicating stability over several earlier cycles, or perhaps a hiatus. Whatever the fate of our hypothesis, we have highlighted the potential of blue-ice moraines to elucidate ice-sheet history. Since they occur widely in Antarctica, they justify closer attention.

Finally, the hypothesis, if substantiated, provides a means of identifying the exact limits of nunataks that remained free of ice during glacial cycles. The existence of such permanently ice-free areas for hundreds of thousands and even tens of millions of years in Antarctica has been postulated by biologists, who find that there is evidence of long-term survival of species, often in discrete locations (Convey *et al.*, 2009). It would be a major step forwards to be able to identify the location and age of exposed nunataks on geomorphological grounds and then to compare the results with those emerging from the biology.

## **Acknowledgements**

The research was funded by the UK Natural Environment Research Council. We acknowledge the contribution of SUERC, where the AMS analyses were carried out and the work of Elaine McDougall (Edinburgh) who prepared many samples. Antarctic Logistics and Expeditions provided the logistic support expertly.

## **Cosmogenic nuclide analysis: methods**

Samples were processed at The University of Edinburgh's Cosmogenic Isotope Laboratory following procedures adapted from the methods of Bierman *et al* (2002) and Kohl and Nishiizumi (1992). A reference 0.25 mg 'spike' of commercially available non-cosmogenic  $^9\text{Be}$



carrier solution (Scharlab Be solution; concentration  $984 \pm 2$  ppm) was added to each sample and the corresponding blank. The  $^{10}\text{Be}/^9\text{Be}$  ratios were measured at the Scottish Universities Environmental Research Centre (SUERC) AMS laboratory (Freeman et al., 2004). The measured sample concentrations were corrected by full chemistry procedural blanks, which had  $^{10}\text{Be}/^9\text{Be}$  ratios ranging from  $5.96 \times 10^{-15}$  to  $1.67 \times 10^{-14}$ . This ratio was subtracted from the Be isotope ratios of the samples, with blank-corrected  $^{10}\text{Be}/^9\text{Be}$  ratios of the samples ranging from  $9.45 \times 10^{-15}$  to  $9.05 \times 10^{-12}$ . Final analytical error in concentration ( $\text{at.g}^{-1}$ ) is derived from a sum in quadrature of the standard mean error of the measured AMS ratio and 2% in the Be ‘spike’ assay (measured by ICP-AES).

Apparent exposure ages (Table 1) were generated using a  $^{10}\text{Be}$  production rate scaled to sea level high latitude (SLHL) in Antarctica using the CRONUS-Earth Online calculator of Balco et al. (2008). We used the following version: Wrapper script 2.2; Main calculator 2.1; Constants 2.2.1; Muons 1.1. The exposure ages outlined in Table S1 are based on the constant production rate model and using the Antarctic pressure scaling model (Stone, 2000; Lal, 1991). At high latitude and the altitude range of our sampling sites (700-1400 m), the pressure dependent altitude scaling of all currently used scaling factors differ marginally ( $< 3\%$ ) from each other. Therefore our calculated ages are not significantly affected by the choice of the scaling model used. Sample thickness (self-shielding) corrections were calculated using an attenuation coefficient of  $160 \text{ g cm}^{-2}$  and a rock density of  $2.65 \text{ g cm}^{-3}$ . We report full external uncertainties in single-nuclide exposure ages, representing full propagation of the production rate uncertainty together with the AMS measurement errors defined above.

## References

Ackert, R. P., Barclay, D.J., Borns, H.W., Calkin, P.E., Kurz M.D., Fastook, J.L., Steig, E.J. 1999. Measurement of ice sheet elevations in interior West Antarctica. *Science* 286, 276-280.

Anderson, J.B., Shipp, S.S., Lowe, A.L., Wellner, J.S., Mosola, A.B., 2002. The Antarctic Ice Sheet during the Last Glacial Maximum and its subsequent retreat history: a review. *Quat. Sci. Rev.*, 21, 49-70.

Bamber, J.L., Riva, R.E.M., Vermeersen, B.L.A., LeBrocq, A.M. 2009. Reassessment of the Potential Sea-Level Rise from a Collapse of the West Antarctic Ice Sheet. *Science*, 324 (5629), 901-903.

Balco G., Stone J., Lifton N., Dunai T., 2008. A simple, internally consistent, and easily accessible means of calculating surface exposure ages and erosion rates from Be-10 and Al-26 measurements. *Quaternary Geochronology* 3, 174-195.

Bentley, M.J.B., Fogwill, C.J., Le, Brocq, A., Hubbard, A.L., Dunai, T.J., Sugden, D.E., 2010 Deglacial history of the West Antarctic Ice Sheet in the Ellsworth Mountains. *Geology*, 38, 411-414.

Bintanja, R., 1999. On the glaciological, meteorological and climatological significance of Antarctic blue ice areas. *Rev. of Geophys.*, 37, 337-359.

Bierman, P.R., Caffee, M.W., Davis, P.T., Marsella, K., Pavich, M., Colgan, P., Mickelson, D., and Larsen, J., 2002. Rates and timing of earth surface processes from in situ-produced cosmogenic Be-10, Beryllium. *Mineralogy, Petrology, And Geochemistry, Volume 50: Reviews In Mineralogy & Geochemistry: Washington, Mineralogical Soc America*, p. 147-205.

Casassa, G. Rivera, A., Acuna, C., Brecher, H., Lange H. 2004. Elevation change and ice flow at Horseshoe Valley, Patriot Hills, West Antarctica. *Ann. Glaciol.* 39, 20-28.

Convey, P., Stevens, M.I., Hodgson, D.A., Smellie, J.L., Hillenbrand, C-D., Barnes, D.K.A., Clarke, A., Pugh, P.J.A., Linse, K., Craig Cary, S., 2009. Exploring biological constraints on the glacial history of Antarctica. *Quat. Sci. Rev.*, 28, 3035-3048. doi:10.1016/j.quascirev.2009.08.015.

Conway, H., Hall, B.L., Denton, G.H., Gades, A.M., Waddington, E.D., 1999. Past and future grounding-line retreat of the West Antarctic Ice Sheet. *Science*, 286, 280-283.

Dahe, Q., Petit, J.R., Jouzel, J., Stievernard, M., 1994. Distribution of stable isotopes in surface snow along the route of the 1990 International Trans-Antarctic Expedition. *J. Glaciol.* 40, (134), 107-118.

Fink, D., et al., 2006. Pleistocene deglaciation chronology of the Amery Oasis and Radok Lake, Antarctica. *Earth Planet. Sci. Lett.* 243, 229-243.

Freeman, S. et al. (2004) [A new environmental sciences AMS laboratory in Scotland. Nuclear Instruments and Methods in Physics Research Section B: Beam Interactions with Materials and Atoms](#), 223-224. pp. 31-34. ISSN 0168-583X.

Fogwill, C.J., Bentley, M.J., Sugden, D.E., Kerr, A.R., Kubik, P.W., 2004 Cosmogenic nuclides  $^{10}\text{Be}$  and  $^{26}\text{Al}$  imply limited Antarctic ice sheet thickening and low erosion in the Shackleton range for >1 Myr. *Geology*, 32, 265-8.

Genthon, C., Braun, A., 1995. ECMWF analyses and predictions of the surface climate of Greenland and Antarctica. *J. Climate*, 8 (10), 2324-2332.

Graham, A.G.C., Larter, R.D., Gohl, K., Hillenbrand, C-D., Smith, J.A., Kuhn, G., 2009. Bedform signature of a West Antarctic palaeo-ice stream reveals a multi-temporal record of flow and substrate control. *Quat. Sci. Rev.*, 28, 2774-2793.

Hearty, P.J., 1998. The geology of Eleuthera Island, Bahamas: a rosetta stone of Quaternary stratigraphy and sea-level history. *Quat. Sci. Rev.* 17, 333-355.

Hearty, P.J., et al., 2007. Global sea-level fluctuations during the last interglaciation (MIS 5e) *Quat. Sci. Rev.*, 26, 2090-2112.

Hollin, J.T., 1965. Wilson's theory of ice ages, *Nature*, 208, 12-16.

Huybrechts, P., 2002. Sea-level changes at the LGM from ice-dynamic reconstructions of the Greenland and Antarctic ice sheets during glacial cycles, *Quat. Sci. Rev.*, 21, 203-231.

Ivy-Ochs, S., 1996. The dating of rock surfaces using in situ produced  $^{10}\text{Be}$ ,  $^{26}\text{Al}$  and  $^{36}\text{Cl}$ , with examples from Antarctica and the Swiss Alps. PhD Thesis, Zurich, Swiss Federal Institute of Technology, 196 pp.

Kohl, C.P., and Nishiizumi, K., 1992. Chemical Isolation of Quartz for Measurement of In situ-Produced Cosmogenic Nuclides. *Geochimica et Cosmochimica Acta*, v. 56, p. 3583-3587.

Kowalewski, D.E., Marchant, D.R., Levy, J.S., Head, J.W., 2006. Quantifying low rates of summertime sublimation for buried glacier ice in Beacon Valley, Antarctica. *Antarctic Science*, 18 (3), 421-428.

Kopp, R.E., Simons, F.J., Mitrovica, J.X., Maloof, A.C. and Oppenheimer, M. 2009. Probabilistic assessment of sea level during the last interglacial stage, *Nature*, 462, 863-868.

Lal, D., 1991. Cosmic ray labelling of erosion surfaces: in situ nuclide production rates and erosion rates. *Earth Planet. Sci. Lett.*, 106, 381-395.

Mackintosh, A., White, D., Fink, D., Gore, D.B., Pickard, J., Fanning, P.C., 2007. Exposure ages from mountain dipsticks in Mac.Robertson Land, East Antarctica, indicate little change in ice-sheet thickness since the LGM. *Geology*, 35, 551-554.

McCulloch, M.T. Esat, T. 2000. The coral record of the last interglacial sea levels and sea surface temperatures. *Chem. Geol.* 169, 107-129.

Mercer, J.H., 1978. West Antarctic Ice Sheet and CO<sub>2</sub> greenhouse effect: a threat of disaster. *Nature*, 271, 321-5.

Mulvaney R. et al., 2007. A deglaciation climate and ice-sheet history of the Weddell Sea region from the Berkner Island ice core. *Quat. Internat.*, 167-168, 294-295.

Naish, T. and 55 others, 2009. Obliquity-paced Pliocene West Antarctic ice sheet oscillations. *Nature*, 458, 322-329.

Näslund, J.-O., 1992, Blue ice investigations in the Scharffenberg-botnen basin, in: Melander, O. and Lönnroth Carlsson, M., Swedish Antarctic Research programme 1991/92: a cruise report, 48-53, Swed. Polar Res., Soc., 00-00.

Nishiizumi, K., 2004. Preparation of Al-26 AMS standards. *Nuclear Instruments & Methods in Physics Research Section B*, v. 223-24, p. 388-392.

Nishiizumi, K., Imamura, M., Caffee, M.W., Southon, J.R., Finkel, R.C., and McAninch, J., 2007. Absolute calibration of Be-10 AMS standards. *Nuclear Instruments & Methods in Physics Research Section B*, v. 258, p. 403-413.

Pollard, D., DeConto, R.M., 2009. Modelling West Antarctic ice sheet growth and collapse through the past five million years. *Nature*, 458, 329-333.

Pritchard, H.D. et al. 2009. Extensive dynamic thinning on the margins of the Greenland and Antarctic ice sheets. *Nature*, 461, 971-975.

Raynaud, D. et al., 2003. In Earth's Climate and Orbital Eccentricity: the Marine Isotope Stage 11 Question. Eds. Droxler, A.W., Poore, R.Z., Burckle, L.H. American Geophysical Union, 27-40.

Ritz, C., Rommelaere, V., Dumas, C., 2001. Modeling the evolution of Antarctic ice sheet over the last 420,000 years: implications for altitude changes in the Vostok region. *J. Geophys. Res.* 106, 31943-31964.

Rohling, E.J. et al., 2008. High rates of sea-level rise during the last interglacial period. *Nature Geoscience* 1, 38-42.

Scherer, R.P., 1991. Quaternary and tertiary microfossils from beneath Ice stream B – evidence for a dynamic West Antarctic Ice-sheet history. *Glob. Planet. Change*, 90, 395-412.

Schoof, C., 2007, Ice sheet grounding line dynamics: steady states, stability and hysteresis. *J. Geophys. Res.*, 112, doi: 10.1029/2006JF000664.

Shepherd, A., et al., 2001. Inland thinning of Pine Island glacier, West Antarctica. *Science*, 291, 862-864.

Siddall, M., et al., 2003. Sea-level fluctuations during the last glacial cycle. *Nature*, 423, 853-858.

- Sinisalo, A., Moore, J.C., 2010. Antarctic blue ice areas – towards extracting palaeoclimatic information. *Antarctic Science*, 22 (2), 99-115.
- Stone, J.O., 2000. Air pressure and cosmogenic isotope production. *J. Geophys. Res.*, 105, 23,753-23,759.
- Stone, J.O., Balco, G.A., Sugden, D.E., Caffee, M.W., Sass, L.C., Cowdery, S.G., Siddoway, C., 2003. Holocene deglaciation of Marie Byrd Land, West Antarctica, *Science*, 299, 99-102.
- Sugden, D.E., Knight, P.G., Livesey, N., Lorrain, R.D., Souchez, R.A., Tison, J-L., Jouzel, J., 1987. Evidence of two zones of debris entrainment beneath the Greenland ice sheet. *Nature*, 328, 238-241.
- Sugden, D. E., Balco, G., Cowdery, S.G., Stone, J.O., Sass, L.C., 2005 Selective glacial erosion and weathering zones in the coastal mountains of Marie Byrd Land., *Geomorphology*, 67, 317-334.
- Warner, R.C., Budd, W.F., 1998. Modelling the long-term response of the Antarctic ice sheet to global warming. *Ann. Glaciol.*, 27, 161-168.
- Webers, G.F., Craddock, C., Splettstoesser, J.F., 1992. Geological history of the Ellsworth Mountains, west Antarctica, in: Webers, G.F., Craddock, C., Splettstoesser, J.F., *Geology and Palaeontology of the Ellsworth Mountains, West Antarctica*. Geol. Soc. Amer. Memoir, 170.
- Weertman, J., 1974, Stability of the junction of an ice sheet and an ice shelf. *J. Glaciol.* 13, 3-11.
- Whillans, I.M., Cassidy, W.A., 1983. Catch a falling star: meteorites and old ice. *Science*, 222, (4619), 55-57.

Winther, J-G., Jespersen, M.N., Liston, G.E. 2001. Blue-ice areas in Antarctica derived from NOAA AVHRR satellite data. *J. Glaciol.*, 47, 325-334.

Yoshida, M., Ando, H., Omoto, K., Ageta, Y., 1971. Discovery of meteorites near Yamato Mountains, East Antarctica. *Antarctic Record*, 39, 62-65.

## **List of Figures**

Fig. 1. The location of the southern Heritage Range (source: GoogleEarth). Ice flows from the central West Antarctic Ice Sheet dome in the southwest (bottom left) to the Filchner-Ronne Ice Shelf in the northeast (top right). Inset: The wider Antarctic setting.

Fig. 2. Oblique air photograph of Drake Icefall and Soholt Peaks showing two large blue-ice moraines at the escarpment foot and a thinner medial moraine at the junction with Union Glacier. Photo courtesy of the USGS.

Fig. 3. Above. Oblique air photo showing the hooked moraines of the Independence Hills. The Marble Hills are to the left and the Patriot Hills in the background. The Blue ice moraine in the Patriot Hills is on the far side of the mountain block. Photo courtesy of the USGS. Below. Geomorphological map showing the moraines and the location of four  $^{10}\text{Be}$  cosmogenic nuclide exposure dates.

Fig. 4. View down the ice slope to the blue-ice moraine at the foot of the Patriot Hills escarpment. The upper transect in Fig. 5 is across the extensive moraine area in the embayment and the lower transect is 1.5 km to the right.

Fig. 5 Above. Transect across the moraines in the embayment featured in Fig. 4, showing the amplitude, sediment and morphological characteristics and the relationship to dipping debris bands.



Below. Transect across the blue-ice moraine and the interplay with local ice 1.5 km to the northwest of the upper transect.

Fig. 6. Photo of a clast emerging from a folded debris band at the ice surface. The long axis of the stone is parallel to the dip of the debris band. Two similar clasts on the ice surface show no measurable exposure to cosmic rays.

Fig. 7. Beryllium and Aluminium exposure ages of samples on the escarpment front of the Patriot Hills (Aluminium age = second value). The dotted line represents the LGM limit, below which there is a range of ages with many samples having the same co-isotopic exposures ages (within error), implying simple exposure histories. Clasts on the ice have minimum exposure, while weathered clasts at the upper limit with Beryllium ages of  $\sim 400$  kyr require further investigation. See Table 1 for the complete dataset.

Fig. 8. Schematic of the hypothesis of blue-ice formation that best fits the evidence of ice, debris structures and exposure age analysis of deposits on the Patriot Hills escarpment front. Fresh basal debris emerges at the glacier surface by compressive flow in response to surface ablation by katabatic winds accumulates over tens of thousands of years. During glacial cycles the ice thickens and thins in response to sea-level change and deposits moraines on the escarpment front.

Table 1. Cosmogenic nuclide data.

The reported nuclide concentrations measured at SUERC are normalised to NIST SRM-4325 Be standard material with a nominal  $^{10}\text{Be}/^9\text{Be}$  ratio of  $3.06 \times 10^{-11}$  and a half-life of 1.51 Myr, and the Purdue Z92-0222 Al standard material with a nominal  $^{26}\text{Al}/^{27}\text{Al}$  ratio of  $4.11 \times 10^{-11}$  that agrees with Al standard material of Nishiizumi et al. (2004). The  $^{10}\text{Be}$  concentrations were published previously by Bentley et al. (2010). Uncertainties are 1 sigma. Nuclide concentrations include propagated AMS sample/lab-blank uncertainty, 2% carrier mass

uncertainty (Be) and 5% stable  $^{27}\text{Al}$  measurement (ICP-OES) uncertainty. Exposure ages were calculated using the CRONUS-Earth web based calculator (Wrapper script 2.2; Main Calculator 2.1; constants 2.2.1 and muons 1.1)(Balco et al., 2008); the concentrations were therefore re-normalised internally to be consistent with the  $^{10}\text{Be}$  half-life (1.36 Myr) of Nishiizumi et al. (2007). Full external age uncertainties are reported.

Figure 1  
[Click here to download high resolution image](#)

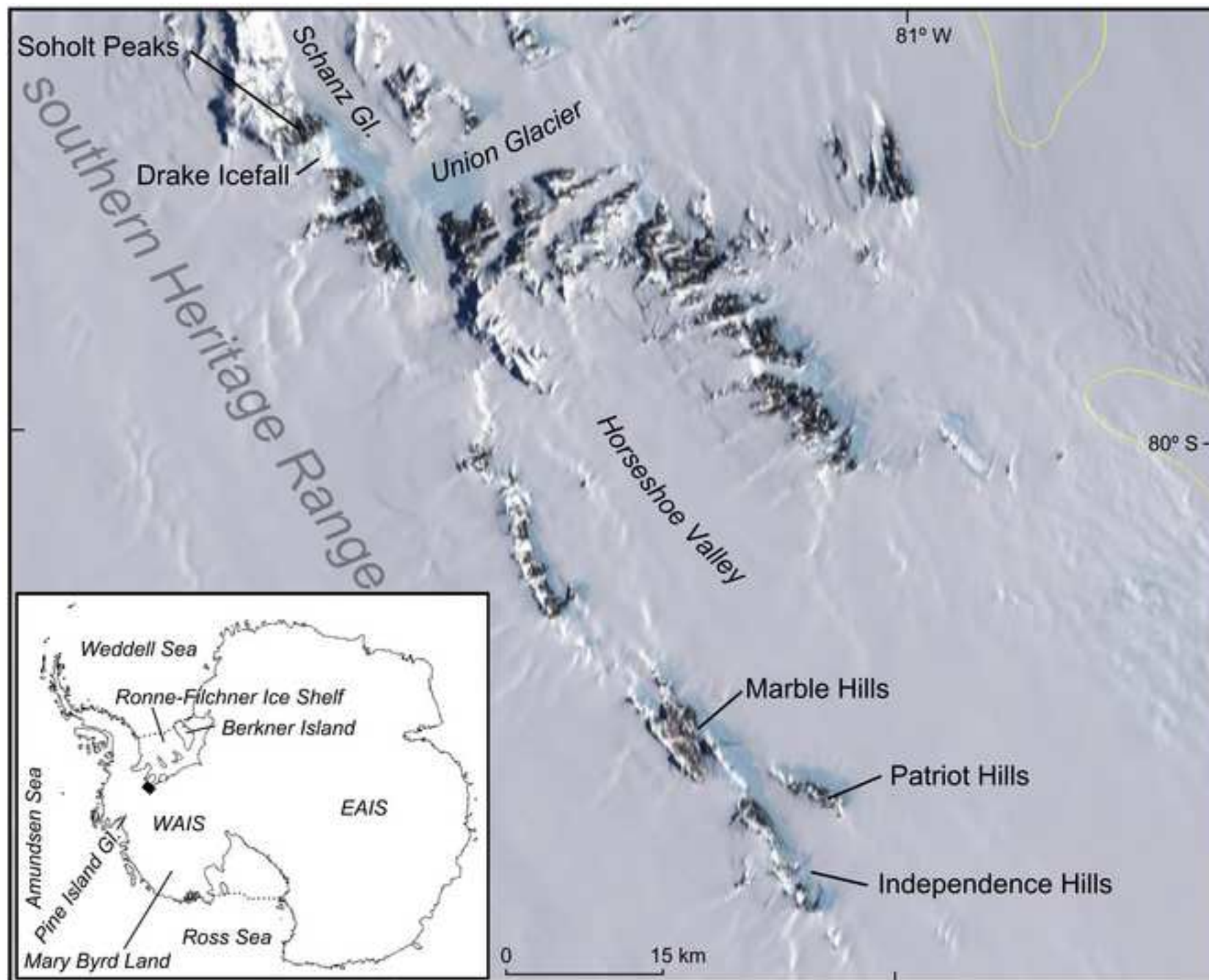


Figure 2  
[Click here to download high resolution image](#)

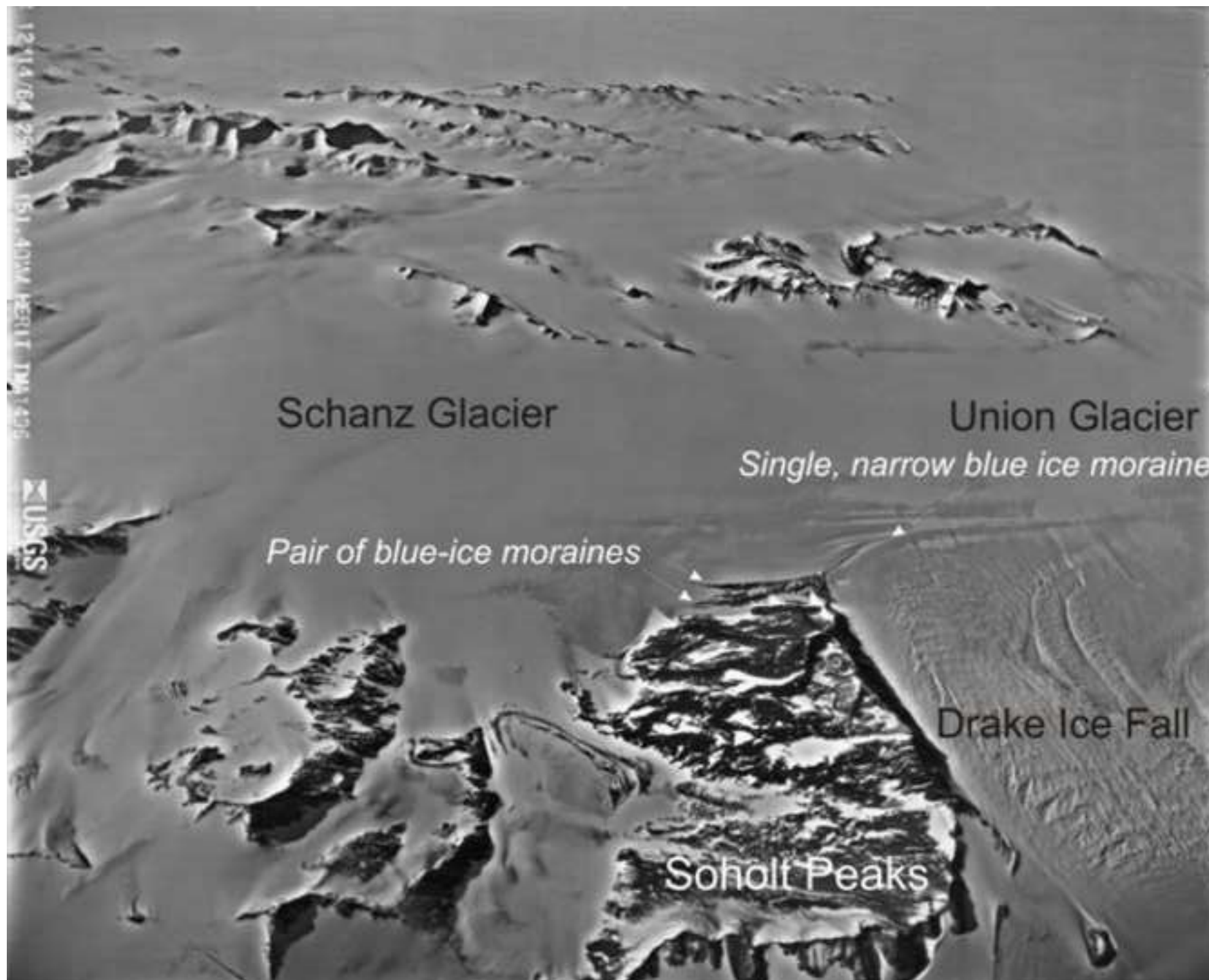


Figure 3a  
[Click here to download high resolution image](#)

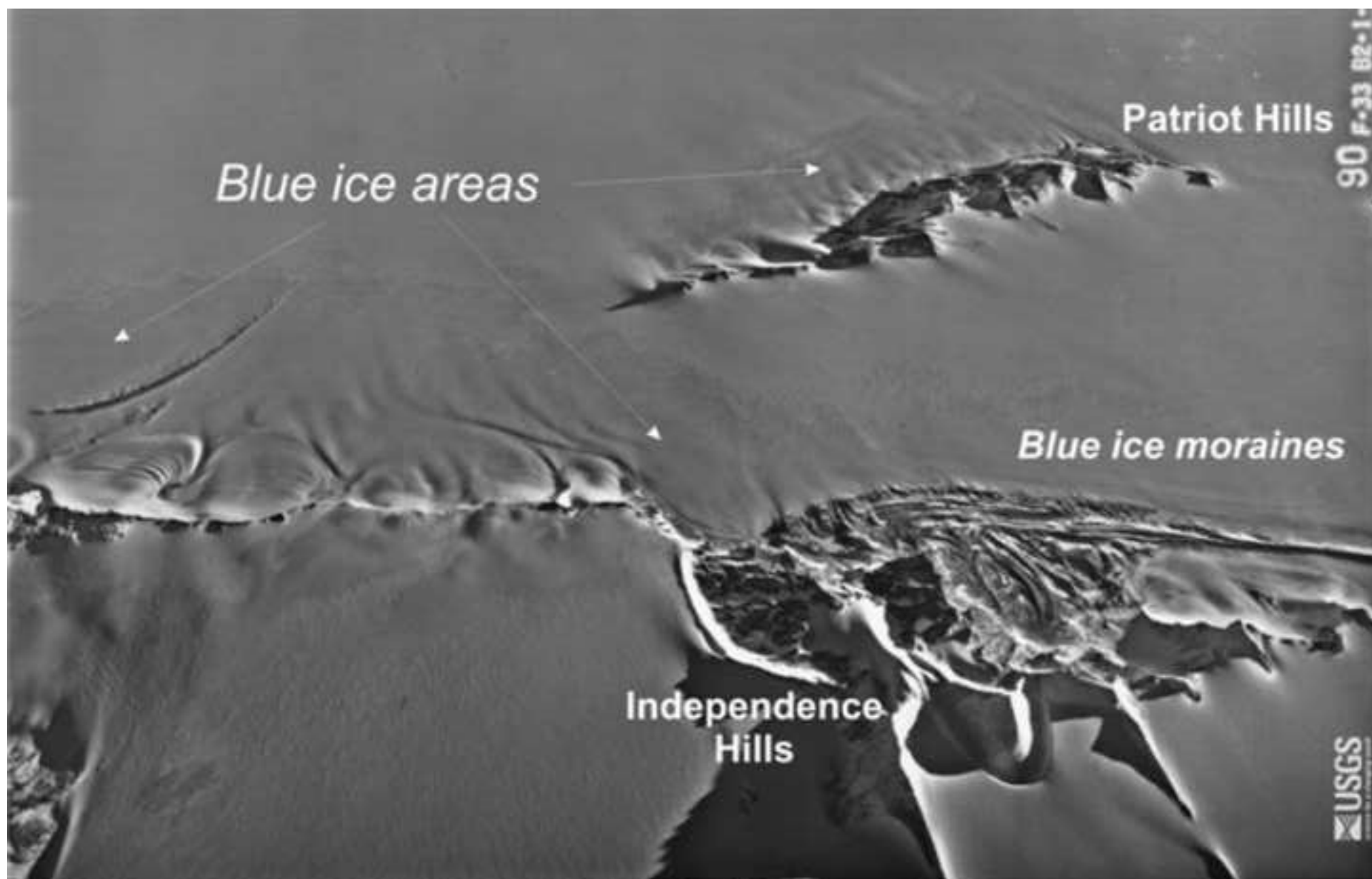




Figure 3b  
[Click here to download high resolution image](#)

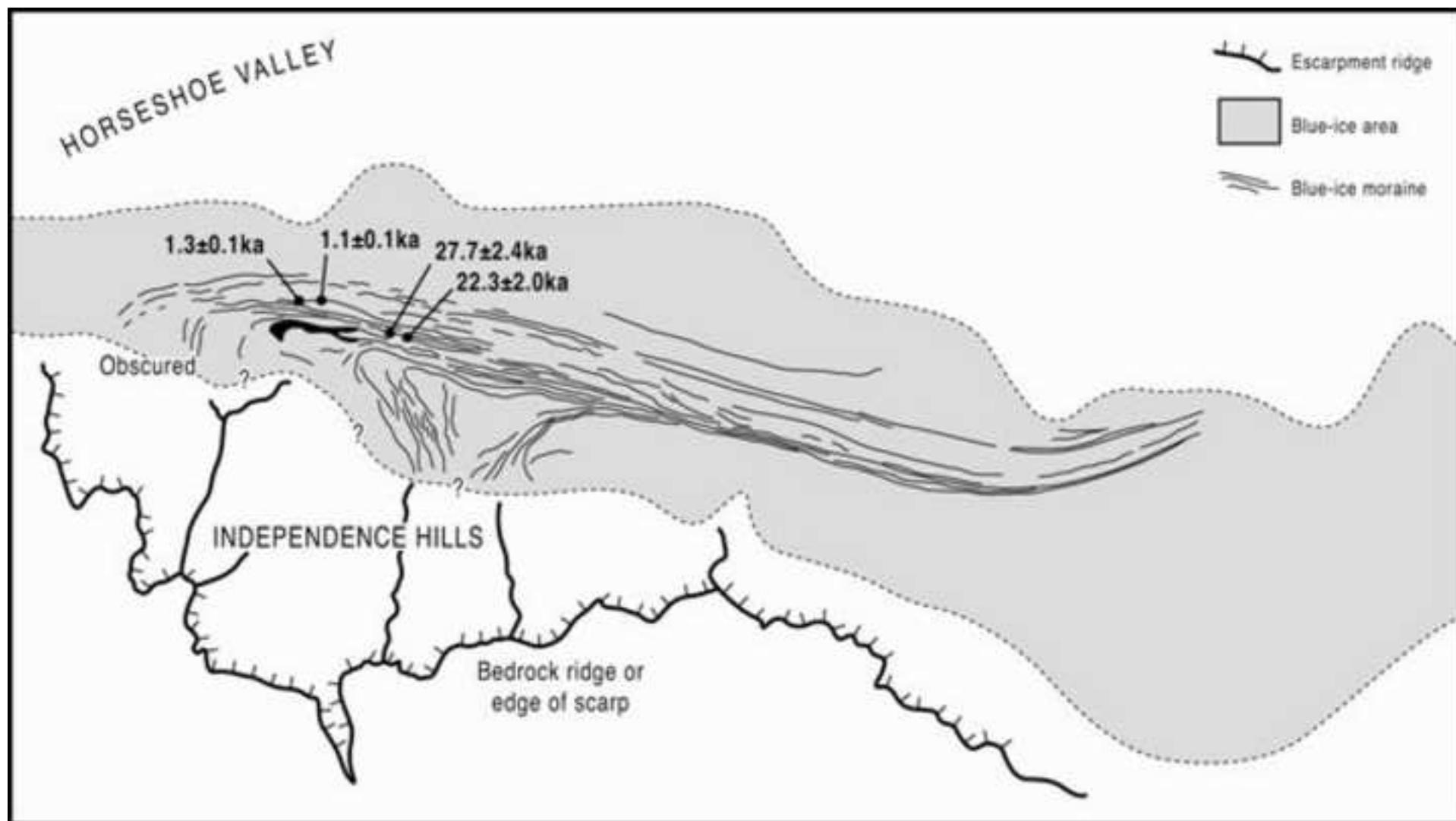


Figure 4  
[Click here to download high resolution image](#)



Figure 5  
[Click here to download high resolution image](#)

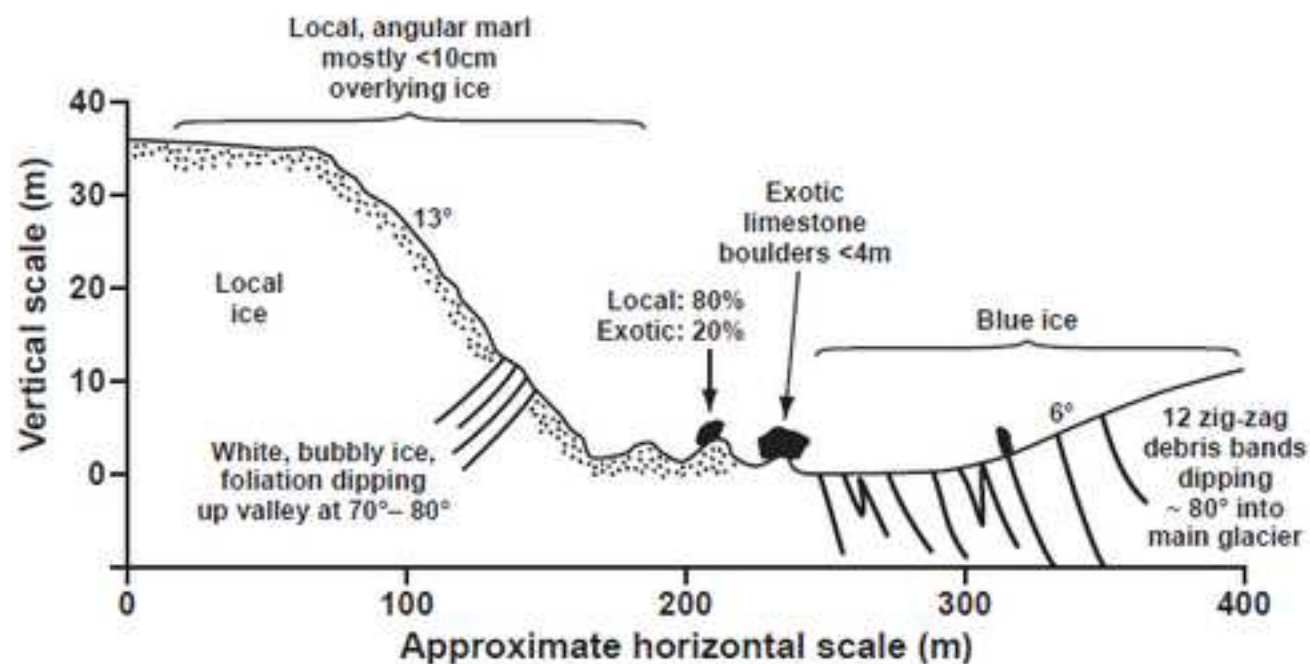
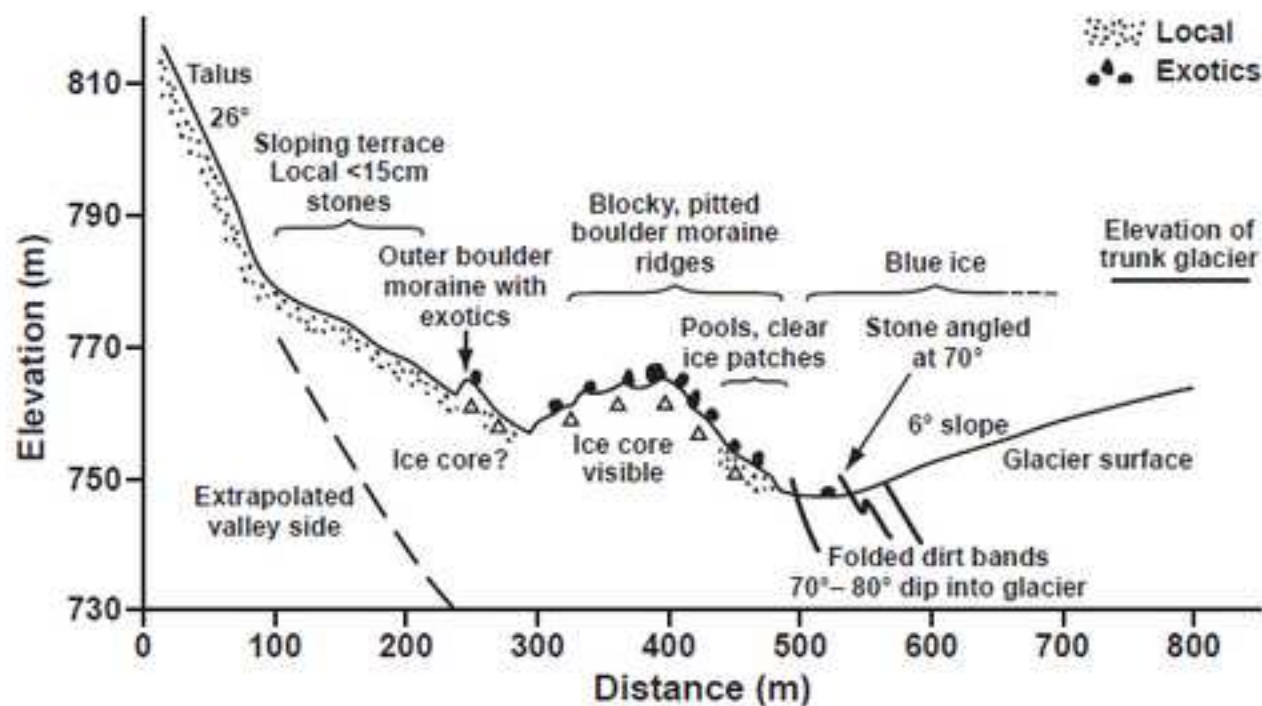




Figure 6

[Click here to download high resolution image](#)



**Figure 7**  
[Click here to download high resolution image](#)

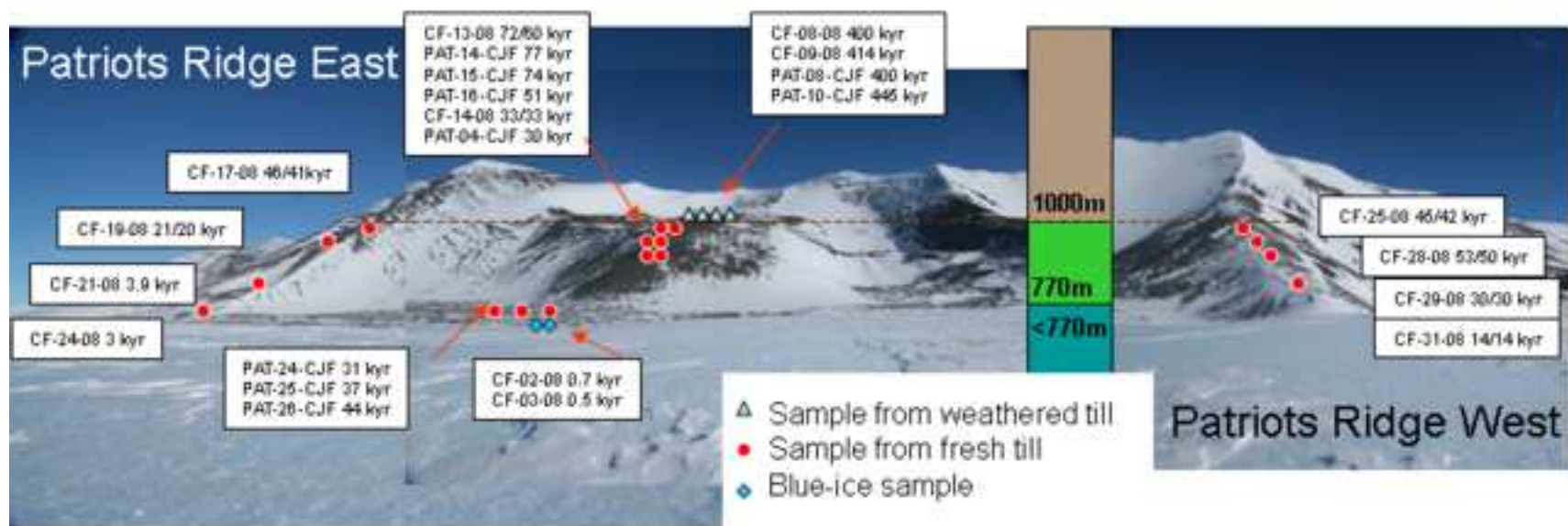


Figure 8  
[Click here to download high resolution image](#)

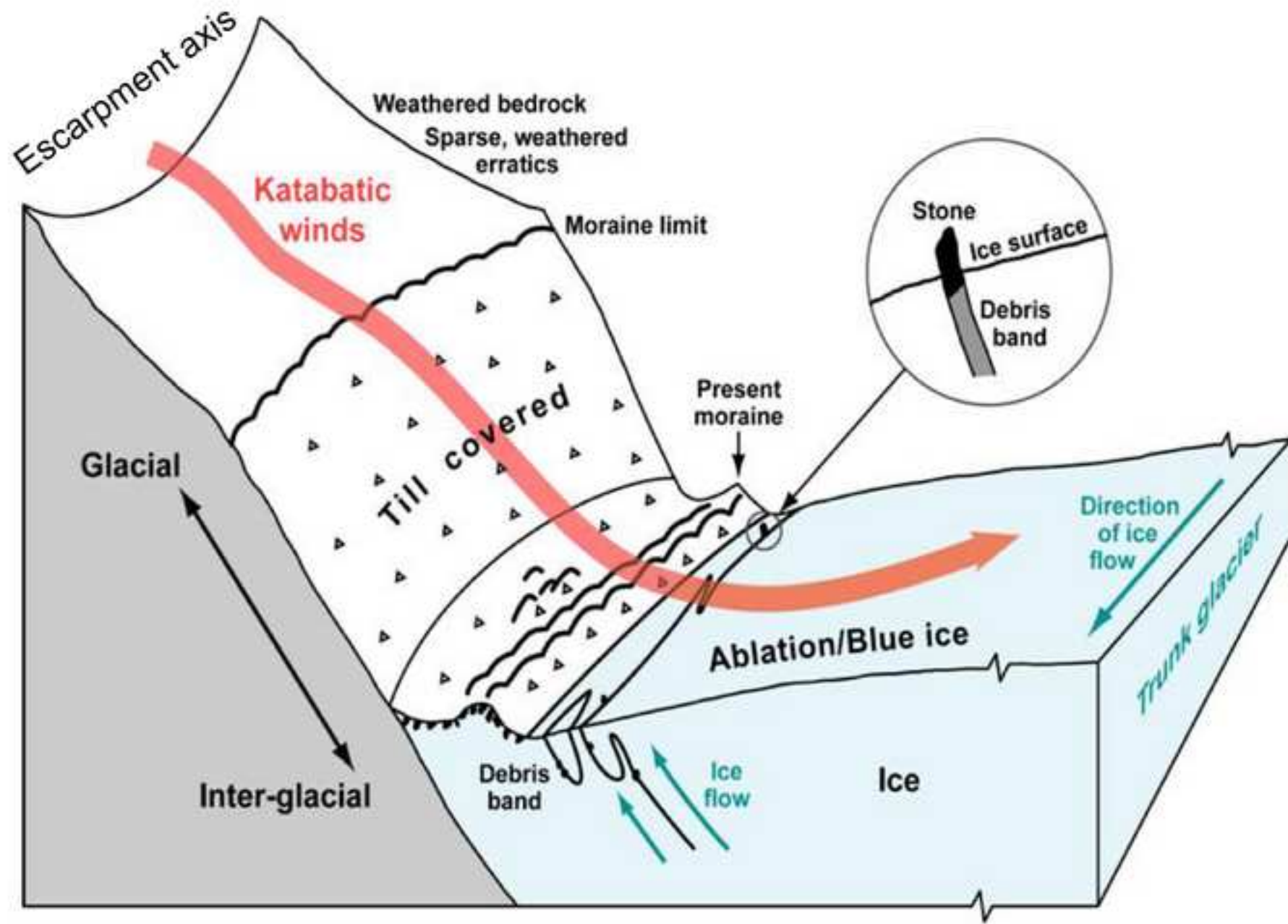


Table 1  
Click here to download Table: BIM\_data table.xls

Sample ID	Latitude (dd)	Longitude (dd)	Sample altitude (m)	Sample thickness (cm)	Topographic shielding	<sup>10</sup> Be concentration (10 <sup>6</sup> atoms/g)	<sup>10</sup> Be concentration error (10 <sup>6</sup> atoms/g)	<sup>26</sup> Al concentration (10 <sup>6</sup> atoms/g)	<sup>26</sup> Al concentration error (10 <sup>6</sup> atoms/g)	<sup>10</sup> Be exposure age (kyr)	<sup>10</sup> Be age uncertainty (kyr)	<sup>26</sup> Al exposure age (kyr)	<sup>26</sup> Al age uncertainty (kyr)
Patriot Hills													
CF-01-08	-80.3263	-81.3345	760	5	0.98	1.67E+05	8.51E+03	7.02E+05	1.25E+05	13.4	1.4	9.1	1.8
CF-02-08	-80.3265	-81.3312	760	5	0.99	9.41E+03	1.33E+03	0.00E+00	0.00E+00	0.7	0.1	--	--
CF-03-08	-80.3268	-81.3269	762	5	0.98	6.19E+03	4.13E+02	0.00E+00	0.00E+00	0.5	0.5	--	--
CF-08-08	-80.3313	-81.3867	1014	5	0.98	5.65E+06	5.47E+04	2.58E+07	1.35E+06	400.1	38.7	310.5	36.8
CF-09-08	-80.3314	-81.3857	1004	5	0.99	5.83E+06	7.19E+04	2.68E+07	1.41E+06	413.6	40.3	324.2	38.8
CF-13-08	-80.3306	-81.3832	989	5	0.97	1.06E+06	1.75E+04	5.40E+06	2.99E+05	71.5	6.4	59.5	6.3
CF-14-08	-80.3306	-81.3652	935	5	0.97	4.76E+05	1.29E+04	2.88E+06	1.64E+05	33.3	3.1	32.8	3.5
CF-17-08	-80.3305	-81.3300	826	5	0.97	5.96E+05	1.60E+04	3.27E+06	1.89E+05	46.0	4.2	41.1	4.4
CF-19-08	-80.3303	-81.3300	816	5	0.97	2.75E+05	6.30E+03	1.55E+06	8.93E+04	21.3	1.9	19.5	2.0
CF-21-08	-80.3295	-81.3267	774	5	0.99	5.02E+04	1.29E+03	0.00E+00	0.00E+00	3.9	0.4	--	--
CF-24-08	-80.3292	-81.3254	761	5	0.97	3.76E+04	5.00E+02	0.00E+00	0.00E+00	3.0	0.3	--	--
CF-25-08	-80.3236	-81.4352	940	5	0.97	6.45E+05	1.64E+04	3.68E+06	2.42E+05	45.1	4.1	41.9	4.7
CF-28-08	-80.3230	-81.4347	879	5	0.97	7.12E+05	1.85E+04	4.16E+06	2.95E+05	52.6	4.8	50.2	5.8
CF-29-08	-80.3224	-81.4341	879	5	0.97	4.08E+05	1.09E+04	2.48E+06	1.55E+05	30.0	2.7	29.6	3.2
CF-31-08	-80.3219	-81.4343	863	5	0.97	1.85E+05	4.25E+03	1.17E+06	7.17E+04	13.7	1.2	14.1	1.5
PAT-04-CJF	-80.3309	-81.3848	933	5	0.97	4.25E+05	1.14E+04	0.00E+00	0.00E+00	29.8	2.7	--	--
PAT-08-CJF	-80.3300	-81.3819	1004	5	0.97	5.54E+06	8.78E+04	0.00E+00	0.00E+00	399.7	39.1	--	--
PAT-10-CJF	-80.3295	-81.3791	1002	5	0.97	6.09E+06	1.08E+05	0.00E+00	0.00E+00	444.9	44.2	--	--
PAT-13-CJF	-80.3279	-81.3389	978	5	0.97	5.25E+06	9.61E+04	0.00E+00	0.00E+00	386.0	37.8	--	--
PAT-14-CJF	-80.3280	-81.3374	968	5	0.97	1.12E+06	2.14E+04	0.00E+00	0.00E+00	77.0	7.0	--	--
PAT-15-CJF	-80.3275	-81.3435	965	5	0.97	1.08E+06	1.46E+04	0.00E+00	0.00E+00	74.4	6.7	--	--
PAT-16-CJF	-80.3285	-81.3538	960	5	0.97	7.40E+05	2.05E+04	0.00E+00	0.00E+00	50.9	4.7	--	--
PAT-18-CJF	-80.3283	-81.3541	774	5	0.97	4.10E+05	9.60E+03	0.00E+00	0.00E+00	33.1	3.0	--	--
PAT-20-CJF	-80.3283	-81.3541	772	5	0.97	9.83E+05	1.06E+04	0.00E+00	0.00E+00	80.3	7.2	--	--
PAT-21-CJF	-80.3282	-81.5026	769	5	0.97	4.10E+05	6.99E+03	0.00E+00	0.00E+00	33.2	3.0	--	--
PAT-24-CJF	-80.3251	-81.5332	777	5	0.97	3.89E+05	8.01E+03	0.00E+00	0.00E+00	31.3	2.8	--	--
PAT-25-CJF	-80.3245	-81.5359	775	5	0.97	4.57E+05	7.20E+03	0.00E+00	0.00E+00	36.8	3.3	--	--
PAT-26-CJF	-80.3235	-81.5416	775	5	0.99	5.61E+05	1.20E+04	0.00E+00	0.00E+00	44.4	4.0	--	--
Marble Hills													
MAR-04-MJB	-80.2614	-82.1700	1246	5	0.99	3.73E+06	9.24E+04	2.13E+07	3.99E+05	205.6	19.6	197.9	19.4
MAR-09-CJF	-80.2631	-82.0985	1305	5	0.99	3.05E+05	2.27E+03	0.00E+00	0.00E+00	15.3	1.3	--	--
MAR-11-CJF	-80.2350	-82.1827	1280	5	0.99	3.05E+05	9.96E+03	0.00E+00	0.00E+00	15.6	1.5	--	--
Independence Hills													
IND-08-CJF	-80.3466	-81.6666	857	5	0.99	1.72E+04	6.86E+02	0.00E+00	0.00E+00	1.3	0.1	--	--
IND-09-CJF	-80.3466	-81.6669	863	5	0.99	1.55E+04	3.65E+02	0.00E+00	0.00E+00	1.1	0.1	--	--
IND-12-CJF	-80.3495	-81.6676	859	5	0.99	3.78E+05	3.12E+03	0.00E+00	0.00E+00	27.7	2.4	--	--
IND-13-CJF	-80.3496	-81.6671	858	5	0.99	3.05E+05	1.99E+03	0.00E+00	0.00E+00	22.3	2.0	--	--

Background dataset for online publication only

[Click here to download Background dataset for online publication only: Supplementary Material.doc](#)